

PERFORMANCE OF AN AERODYNAMIC YAW CONTROLLER MOUNTED ON THE SPACE SHUTTLE ORBITER BODY FLAP AT MACH 10

W. I. Scallion

ABSTRACT

A wind-tunnel investigation of the effectiveness of an aerodynamic yaw controller mounted on the lower surface of a shuttle orbiter model body flap was conducted in the Langley 31-Inch Mach 10 Tunnel. The controller consisted of a 60° delta fin mounted perpendicular to the body flap lower surface and yawed 30° to the free stream direction. The control was tested at angles of attack from 20° to 40° at zero sideslip for a Reynolds number based on wing mean aerodynamic chord of 0.66×10^6 . The aerodynamic and control effectiveness characteristics are presented along with an analysis of the effectiveness of the controller in making a bank maneuver for Mach 18 flight conditions. The controller was effective in yaw and produced a favorable rolling moment. The analysis showed that the controller was as effective as the reaction control system in making the bank maneuver. These results warrant further studies of the aerodynamic/aerothermodynamic characteristics of the control concept for application to future space transportation vehicles.

SUMMARY

A limited wind tunnel investigation of the effectiveness of an aerodynamic yaw controller mounted on the lower surface of a space shuttle orbiter model body flap was conducted in the Langley 31-Inch Mach 10 Tunnel. The tests were conducted at angles of attack of 20° to 40° at zero sideslip for a Reynolds number based on wing mean aerodynamic chord of 0.66×10^6 . The controller consisted of a 60° swept fin mounted perpendicular to the body flap lower surface and yawed 30° to the free stream direction. This configuration represented a triangular-shaped piece of the body flap tip deflected 90° downward for yaw control. The results indicated that the controller was effective in yaw and produced a favorable rolling moment and a nose down pitching moment that could be trimmed out with elevon. The wind tunnel results were used in a three-degree-of-freedom analysis of the initiation of an entry bank reversal at Mach 18. The analysis showed that the controller was as effective as the reaction control system, thus saving about 66 lb of propellant. The findings of this study warrant additional studies of the aerodynamic and aeroheating characteristics of the control concept.

INTRODUCTION

The control of spacecraft during atmospheric entry would ideally be accomplished with movable aerodynamic surfaces. This would avoid the use of

reaction control systems (RCS) with their attendant interaction effects with the flow field and the additional weight of the required propellant. In the practical sense this is difficult because of the lack of effective aerodynamic control in yaw. At high angles of attack, conventional vertical tails are ineffective. Pitch and roll control can be maintained with wing trailing-edge controls although sometimes not without some adverse effects in yaw with aileron deflection. Aerodynamic yaw control can be accomplished with tip fins (ref. 1), but the associated structural and thermal protection system weights may be unacceptable. To date, the practical solution to the problem is a combination of movable aerodynamic surfaces and reaction controls. The reaction controls are already necessary for control out of the sensible atmosphere, and all that is needed is sufficient tankage for the additional propellant. The space shuttle orbiter is a lifting configuration with large aerodynamic surfaces for pitch and roll control that utilizes the aft-located RCS for yaw control during atmospheric entry. The HL-20 Personnel Launch system being studied (ref. 2) would also utilize a combination of aerodynamic control surfaces and RCS for entry control. The use of the reaction control system for entry requires additional propellant to that necessary for on-orbit maneuver control. In the case of the shuttle orbiter, additional contingencies during entry have required increased allocations of RCS propellant, thus reducing that available for on-orbit maneuvers. For this reason, aerodynamic yaw control becomes attractive because it could make more RCS fuel available for on-orbit maneuvers. Admittedly, such a control would result in increased vehicle weight and complexity and this would have to be weighed against the resulting benefit.

The difficulty with aerodynamic yaw control during entry is that the surface must be located in a region of high-energy flow in order to be effective. The most effective location from the standpoint of aerodynamic control is on the exposed lower surface of the vehicle; however, such a location would correspond to severe aerodynamic heating. The control would be continually exposed to this environment, making it extremely difficult to provide sufficient thermal protection. One way to mitigate the effects of this harsh environment is to design the control such that the critical leading edge is exposed only when the surface is deflected for control. Reference 3 explored this idea with a deployable ventral stabilizer on the HL 10 at Mach 6.8. Langley has been studying this concept as a yaw control that can be applied to the HL-20, the shuttle orbiter, or to future spacecraft that are designed for lifting entry. The concept embodies a principle where the controller, located on the lower surface of a vehicle, lies flush with the surface until it pivots about a hinge into the stream for control. The controller could also be an integral part of a body flap wherein the ends of the body flap would move downward about a canted hinge line.

This report discusses the results of a limited wind tunnel study of the aerodynamic effectiveness of the second controller concept located on the body flap of a 0.0075 scale orbiter model. These tests were conducted in the Langley 31-Inch Mach 10 Tunnel for an angle of attack range 20° to 40° at zero sideslip angle with the model body flap at zero deflection. The model was tested with the body flap alone, and with the controller attached representing 90° deflection; the free stream unit Reynolds number was 2.2 million per foot. The results of these tests were used in a preliminary analysis of the effectiveness of the controller in performing the entry into an orbiter bank reversal maneuver at Mach 18.

SYMBOLS

The aerodynamic data are referred to the body axis system (fig. 1). All coefficients are based on the wing reference planform area, the wing mean aerodynamic chord, and the wing span. The moment reference center was located at the nominal vehicle center of gravity, which was 65 percent of the body length from the inner mold line nose.

b	wing span
c	mean aerodynamic chord
C_A	axial force coefficient, Axial force/ $q_\infty S_{ref}$
C_l	rolling-moment coefficient, Rolling-moment/ $q_\infty S_{ref} b$
$C_{l\beta}$	variation of rolling-moment coefficient with sideslip angle, per degree
$C_{l\delta_a}$	variation of rolling-moment coefficient with aileron deflection, per degree
C_m	pitching-moment coefficient, Pitching moment/ $q_\infty S_{ref} c$
C_N	normal-force coefficient, Normal force/ $q_\infty S_{ref}$
C_n	yawing-moment coefficient, Yawing moment/ $q_\infty S_{ref} b$
$C_{n\beta}$	variation of yawing-moment coefficient with sideslip angle, per degree
$C_{n\delta_a}$	variation of yawing-moment coefficient with aileron deflection, per degree
C_p	pressure coefficient, $(p_L - p_\infty)/q_\infty S_{ref}$
C_Y	side-force coefficient, Side force/ $q_\infty S_{ref}$
$C_{Y\beta}$	variation of side force coefficient with sideslip angle, per degree
$C_{Y\delta_a}$	variation of side-force coefficient with aileron deflection, per degree
H	altitude
I_{XX}	moment of inertia about the body longitudinal axis
I_{ZZ}	moment of inertia about the body vertical axis

N_J	number of jets firing
p	rolling angular velocity
p_L	local surface static pressure
p_∞	free stream static pressure
q_∞	dynamic pressure
Re	Reynolds number based on wing mean aerodynamic chord
r	yawing angular velocity
S_{ref}	reference wing planform area
V_∞	free stream velocity
X	longitudinal body axis
Y	lateral body axis
Z	vertical body axis
α	angle of attack
β	angle of sideslip
δ_a	aileron deflection angle, $(\delta_{eL} - \delta_{eR})/2$
δ_{BF}	body flap deflection angle, positive, trailing edge down
δ_e	elevon deflection angle, positive, trailing edge down
δ_y	yaw controller deflection angle
Φ	roll angle about the body axis

Subscripts

L	left
R	right

CONTROL CONCEPT

The concept of the yaw controller as applied to the orbiter is shown in figure 2. The body flap planform would be modified by making the ends of the body flap parallel to the vehicle x-axis (trailing edge span equal to span at hinge line) to provide more area for the controls. As shown in the figure, the tips of the body flap would deflect individually about canted hinges (canted 30° in the present case) to provide a right or left yaw motion. Because of the nature of the bank maneuvers the orbiter uses during entry, these controls would be used intermittently in the same manner as the yaw RCS to initiate and terminate the maneuvers. Although the control could be deflected to intermediate deflections, it is intended to be deflected fully (90°) for the bank maneuvers. As can be seen in the three-view sketch in figure 2, the outboard edge of the body flap becomes the leading edge of the control with a sweep of 60° when fully deflected to 90° .

APPARATUS AND TESTS

The Langley 31-Inch Mach 10 Tunnel expands heated dry air through a three-dimensional, contoured, water-cooled nozzle into a 31-inch square test section. The nominal test Mach number is 10. The tunnel operates in the blowdown mode with run times ranging from 60 to 120 sec. The air is heated to approximately 1850°R by an electrical resistance heater with reservoir pressures up to approximately 1500 psia. Models are supported on a hydraulically-operated, sidewall-mounted injection system. This tunnel and its capabilities are described in more detail in reference 4.

A 0.0075 scale model with the outer mold lines corresponding to those of the current flight orbiters was used in the present tests. A three-view sketch of the model is shown in figure 3. The model was equipped with elevons that could be deflected by means of hinge-line brackets and replaceable body flaps machined for different deflections. Since the present study was secondary to a test with this model that was being conducted at the same time, only the body flap with zero deflection was available for modification. A single control representing a 90° deflection was fabricated and attached to the body flap underside with machine screws. A drawing of the control is shown in figure 4 and a photograph of the model underside with the control attached is shown in figure 5. The deflected control is triangular in planform with a leading edge sweep of 60° . The planform area is 0.56 percent of the wing reference area.

The force and moment tests were conducted for an angle-of-attack range of 20° to 41° at zero sideslip angle. The model was tested with the body flap alone (at zero deflection) and with the control representing 90° deflection attached, at a unit Reynolds number 2.2 million per foot (0.66×10^6 based on the wing mean aerodynamic chord). An oil-flow visualization of the lower surface with the control attached was run at $\alpha = 40^\circ$ and recorded with a conventional camera. The force and moment measurements were obtained from a six-component, water-cooled internal strain gage balance. Balance internal temperatures were monitored by two thermocouples installed in the surrounding water jacket. The calibration accuracy is 0.5 percent of the design load rating for each of the six components, and the balance-related uncertainties in the coefficients are listed below:

C _N	C _A	C _Y	C _m	C _n	C _l
±0.0095	±0.0019	±0.00096	±0.0016	±0.00014	±0.00027

The moment coefficient uncertainties include the uncertainties in the force coefficients used in the moment transfer equations. The force and moment data were corrected for weight tares, and angle of attack was corrected for sting and balance deflection under load.

FORCE AND MOMENT TEST RESULTS

The force and moment data are presented in figure 6, and the incremental coefficients resulting from the yaw controller at 90° deflection are given in figure 7. Figure 6(d) shows a large offset in C_Y with the basic model without the controller. The cause of this bias was investigated; several test runs were conducted with the model in different facilities with different balances with the same resulting offset in C_Y . It was concluded that the model was not symmetric, and measurements of the model geometry were subsequently made but the data have not been analyzed. However, the repeatability of the data indicated that the model asymmetries would not affect the incremental values obtained with the controller. Installation of the yaw controller deflected 90° produced a small increase in normal force accompanied by a negative increment in pitching moment (fig. 6(a)), that indicates an increase in pressure on the lower surface of the model in the region of the body flap. This is supported by the oil flow visualization in figure 8 which shows a line of demarcation that originates at the apex of the controller and sweeps across the body flap to the trailing edge of the left half of the flap. The turning of the flow ahead of this line indicates a higher pressure in the region behind the line. As shown in figure 7, the yaw controller produced yawing moment and side force increments that increased with angle of attack. A simple calculation of the pressure coefficient on the windward surface of the controller based on ΔC_Y at $\alpha = 40^\circ$ and assuming that the load is evenly distributed, produced a value of C_p of 1.623 or about 89 percent of the stagnation pressure at the nose of the model, which indicates that the control is highly loaded. This is also indicative of high aerodynamic heating on the controller. The rolling moment coefficient produced by deflection of the controller (fig. 7) is about half of the yawing moment and is in a favorable direction. This relationship between the yawing and rolling moments indicates that the control, if sufficiently effective, could produce a coordinated turn when used in conjunction with the ailerons. Although the increment in pitching moment coefficient produced by the controller is sizable ($\Delta C_m = -0.0189$), and causes the vehicle to be out of trim, the data of reference 5 indicate that it can be trimmed out with -5° elevon deflection. A great deal of the moment can be trimmed with the body flap itself, but the level of trim available depends upon the initial body flap deflection. In the present case, with the body flap initially at zero deflection, the full up position ($\delta_{BF} = -11.7^\circ$) would produce a ΔC_m of 0.015.

The controller, when deflected to 90° , produced a 16 percent increase in axial force coefficient (fig. 6(b)) at all angles of attack tested. The effect of this increase in axial force on the performance of the vehicle (untrimmed) is shown in figure 6(c) to be relatively small (a 3 percent decrease in L/D at $\alpha = 20^\circ$).

ANALYSIS AND DISCUSSION

The aerodynamic data have shown that the yaw controller produces a yawing moment without undue adverse effects on the other aerodynamic parameters. It must be established that the control has sufficient effectiveness to adequately maneuver the vehicle. A first order estimate of this can be obtained by comparing the control output to that of the side-firing reaction control system thrusters. The effectiveness of the yaw controller is compared to that of one yaw thruster for a nominal entry trajectory in figure 9. A single yaw thruster produces a vacuum thrust of about 870 lbf. This decreases with altitude, but for the range of altitudes considered (100,000 ft - 255,000 ft), this decrease is negligible. The average yawing moment produced by the thruster is 33,282 ft lb. Dividing this number by $q_\infty S_{ref} b$ for the free stream conditions at the given flight Mach number and correcting the result by applying the interaction yawing moment coefficient for the same conditions gives a reasonable value of the coefficient for a single thruster. The free stream conditions were taken from the nominal reference entry trajectory presented in reference 5.

The yaw controller effectiveness was obtained for Mach 10 only; these data are presented in figure 9 as a function of Mach number. Some justification for this can be found by assuming that the variation of yaw controller effectiveness with Mach number is similar to that of the downward-deflected body flap. Both controls are deflected downward into the same flow field. Reference 5 shows that the downward-deflected body flap effectiveness is unchanged between Mach 20 and Mach 8 at $\alpha = 40^\circ$. At Mach 5, the effectiveness increases about 18 percent at $\alpha = 25^\circ$.

The yaw thruster produces a constant force that is independent of the changing dynamic pressure and therefore, the yawing moment coefficient produced by the thruster decreases as the dynamic pressure increases during entry. The aerodynamic yaw controller has a constant yawing-moment coefficient throughout the hypersonic portion of the entry. At Mach numbers less than 10, the yaw control effectiveness decreases because of the decreasing angle of attack in this portion of the entry. As can be seen in figure 7, the effectiveness of the control becomes less at lower angles of attack. Figure 9 shows that at about Mach 22, the yaw controller effectiveness is equal to that of one yaw thruster and is equivalent to two yaw thrusters at Mach 16. Most of the entry bank maneuvers are accomplished with the part-time use of four thrusters to provide yaw acceleration. The yaw controller can provide the same angular momentum, but would obviously take a longer time. Note that the rolling moment produced by the yaw thruster is adverse, whereas the yaw controller produces a favorable rolling moment. With this relationship, a coordinated turn can be accomplished with aerodynamic controls.

The orbiter bank maneuver about the velocity vector requires a combination of yaw and roll about the respective body axes to maintain the desired angle of attack

during the maneuver. Because the ailerons, when deflected for roll, produce a yawing moment in the opposite direction, the yaw thrusters were required to initiate the bank maneuver. The yaw thrusters produce a yaw rate and a small sideslip angle β . This β generates a rolling moment in the direction of the turn because of the favorable effective dihedral parameter $C_{l\beta}$. The ailerons are used for turn coordination and directional trim.

In order to establish the feasibility of making a bank maneuver using only aerodynamic controls, an analysis was conducted with a combination of the aerodynamic yaw controller and the ailerons. The STS-1 entry flight data (ref. 6) were chosen for the analysis.

The STS-1 entry trajectory showing the bank maneuvers and angle of attack versus time as taken from reference 6 is presented in figure 10. As in all orbiter entries, five bank maneuvers or S-turns are made before reaching the landing area. The first bank maneuver is made where the dynamic pressure is low (12 psf in the present case) and a bank maneuver initiation at this point with the aerodynamic controls would require a considerable length of time. The bank reversal at Mach 18 (maneuver 2) was chosen because the dynamic pressure was sufficiently high. The altitude at this point was 209,000 ft, the relative velocity was 18,477.2 ft/sec, the dynamic pressure was 70.266 lb/ft², and the angle of attack was 40°. At these conditions, the yaw controller is about 1.6 times as effective as one yaw thruster (see fig. 9). The wind tunnel data were referenced to a c.g. position of 65 percent of the reference body length and the STS-1 flight c.g. was at 66.55 percent. The resulting shorter control moment arm required an adjustment in the yaw controller effectiveness, $\partial C_N / \partial Y$, $\partial C_M / \partial Y$, and in the value of $C_{N\beta}$ taken from reference 5. The vehicle and trajectory parameters and the aerodynamic coefficients used in the analysis are given in table I. The aerodynamic data consist of the yaw controller increments taken from figure 7 at $\alpha = 40^\circ$ (with the signs reversed to match the maneuver direction), and the orbiter vehicle stability and control parameters taken from reference 5, with $\partial C_N / \partial y$, $\partial C_M / \partial Y$, and $C_{N\beta}$ adjusted for the change in c.g. location to that of STS-1.

The analysis consisted of utilizing the above mentioned data in the lateral 3-degree-of-freedom equations of motion in yaw, roll, and side slip. It was assumed that the yaw controller takes 2 seconds to fully deflect to 90°, and 2 seconds to retract to 0°. Since data are only available for 90° deflection, the transient aerodynamics were modeled by modifying the coefficient values at 90° deflection by the sine-squared of the intermediate deflection angle. It was mentioned earlier that the rolling-moment coefficient was about one-half the yawing moment coefficient for the deflected yaw controller. However, the yaw moment of inertia is 8.15 times the roll moment of inertia; therefore, when the controller is deflected, the vehicle will accelerate in roll four times faster than in yaw. Because of this it was necessary to modulate the roll rate by deflecting the ailerons. In making a bank maneuver about the velocity vector at a constant angle of attack, the vehicle must maintain a constant ratio of roll to yaw that is a function of angle of attack. At 40° angle of attack, that ratio is 1.192. The aileron deflection was calculated to maintain this ratio of roll to yaw angular velocity during the entry into the maneuver. The elevon deflection required to maintain longitudinal trim during the maneuver was calculated, but it had no bearing on the calculation of the motions. The constant values of the aileron derivatives were adjusted for an average

elevon deflection between 0° and -5° . The equations of motion were programmed in an open-loop mode, and, therefore, several cases were run to obtain convergence on a roll rate equivalent to the final roll rate of the flight case (approximately $-4^\circ/\text{sec}$). In each case, the elapsed time for the controller at 90° deflection was varied until the desired roll rate was obtained. The calculation of the motions was a simple direct summation process over time intervals of 0.10 second.

The results of the analytical calculations are compared to the flight case in figure 11, where the initial entry into the Mach 18 bank reversal (maneuver 2, fig. 10) is presented as a function of time. This figure shows the first 8 seconds of the maneuver from initiation of the motion to where the steady state roll rate is established. In the total maneuver, these steady state motions are maintained until the desired bank angle is reached (about 30 seconds), and the reverse process takes place to arrest the motion. The curves on the left show the control actions and those on the right show the resulting attitude and motions. In the flight case (the solid line), the left side-firing yaw thrusters are fired (upper left in the figure) and the ailerons move to counter the initial adverse roll from the thrusters. Note that 4 thrusters are firing most of the time. Only at the end does the number drop to 3 and then 2. The sideslip angle β builds up and the favorable dihedral effect (negative value of $C_{l\beta}$) causes the vehicle to roll. The roll rate builds up to a slight overshoot and the aileron reverses to moderate this. The roll rate is established in about 5 seconds.

The yaw controller (circular symbols) also shown in the upper left in figure 11 is deflected to 90° and remains there for 4 seconds and then goes to 0° , for a total elapsed time of 8 seconds. The aileron deflects positively to about 1° to modulate the excess roll moment generated by the yaw controller. The positive aileron is desirable because the negative $C_{n\delta_a}$ reinforces the yawing moment of the controller. On the right, the roll rate, p , builds up to nearly the same as the flight roll rate and the yaw rate builds up proportionately. The sideslip angle β remains very nearly zero (maximum value is 0.024°) which confirms that the ratio of proportionality between the yaw and roll rates is correct, and the angle of attack will be maintained close to the desired 40° . The sequence shown in figure 11 shows that the yaw controller, in conjunction with the ailerons can initiate a bank reversal as well as the RCS/aileron combination with the advantage that no RCS propellant was expended. At Mach 18, the time required to initiate the maneuver was longer by 3 seconds, primarily because of the time allotted for deflecting and retracting the controller; however, succeeding bank maneuvers will require less time to initiate because the dynamic pressure is higher (see fig. 10). The total flight maneuver required an expenditure of approximately 66 lbs of RCS propellant. This includes the initiation and termination of the maneuver. Three other bank reversals were made during the STS-1 entry subsequent to the Mach 18 bank reversal (see fig. 10). If, in addition to the Mach 18 maneuver, those three could be made with aerodynamic controls, the total RCS propellant saved for on-orbit use would be approximately 198 lb.

With only Mach 10 data in-hand, it cannot be predicted with certainty that the controller will function as well at the lower Mach numbers. Additional wind tunnel tests are needed to determine the effects of Mach number, angle of attack, body flap deflection, boundary layer transition, and high temperature real-gas phenomena on the control characteristics. At the higher Mach numbers, the aerodynamic heating of the

control and the body flap needs to be determined before the applicability of the control concept to lifting entry vehicles can be established. Subsequent bank maneuvers at the lower Mach numbers (below Mach 10), should produce less severe heating on the control, however, the loads at the higher dynamic pressures will increase, both on the control and the body flap. The calculated side load on the controller and body flap (based on the Mach 10 data) is shown as a function of Mach number in figure 12. As can be seen, the side load doubles from Mach 18 to Mach 4.7. The limited test reported herein did not address the effects of body flap and intermediate control deflections on the characteristics and loads of the control. It is also noted that the use of the yaw controller on the shuttle orbiter would probably result in an increase in weight and aft c.g. movement, and the benefits would have to be assessed against this. The present study has shown that the yaw controller concept is potentially useful for lifting entry vehicle configurations such as the shuttle orbiter, the HL-20, and advanced space vehicle concepts. This warrants further investigation of the factors discussed above.

CONCLUDING REMARKS

The results of a limited wind tunnel investigation at Mach 10 of the effectiveness of an aerodynamic yaw controller mounted on the lower surface of a space shuttle orbiter model body flap indicated that the controller was effective in yaw and produced a favorable rolling moment. The effectiveness of the controller decreased as angle of attack decreased from 40° to 20°. The control also produced a nose-down pitching moment that could be controlled with -5° elevon deflection. The effectiveness of the control was equivalent to that of one RCS yaw thruster at the angle of attack and dynamic pressure for entry flight at Mach 22. This equivalence increased to two at the increased dynamic pressure at Mach 16.

An analysis of the control as applied to an STS-1 bank reversal at Mach 18 showed that the control was as effective as the yaw RCS thrusters in performing the maneuver although slightly more time was required. Use of the controller in this maneuver would save about 66 lb of RCS propellant.

REFERENCES

1. Powell, R. W., and Freeman, D. C., Jr.: Application of a Tip-Fin Controller to the Shuttle Orbiter for Improved Yaw Control. AIAA Journal Guidance, Control, and Dynamics, Vol. 5, No. 4, pp. 325-329, July 1982.
2. Powell, Richard W.: Six-Degree-of-Freedom Guidance and Control-Entry Analysis of the HL-20. AIAA Journal of Spacecraft and Rockets, Vol. 30, No. 5, pp. 537-542, September 1993.
3. Ladson, Charles L.: Aerodynamic Characteristics of a Manned Lifting Entry Vehicle at a Mach Number of 6.8. NASA TM X915, February 1964.
4. Miller, C. G., III: Hypersonic Aerodynamic/Aerothermodynamic Testing Capabilities at Langley Research Center. AIAA-92-3937, July 1992.

5. Anon: Operational Aerodynamic Design Data Book, Vol. II, Orbiter Vehicle, Space Division, Rockwell International Report No. STS 85-0118-2, November 1991.
6. Office of Manned Vehicles, AFFTC: Evaluation of the Space Shuttle Orbiter First Orbital Flight. AFFTC-TR-81-21, July 1981 .

Table I. - Variables Used in the 3-D Analysis

Aerodynamic Parameters

$\Delta C_l (\delta_y = 90^\circ) =$	-0.00199	$C_{l\beta} =$	-0.0017
$\Delta C_m (\delta_y = 90^\circ) =$	-0.0184	$C_{n\delta_a} =$	-0.00041
$\Delta C_n (\delta_y = 90^\circ) =$	-0.003902	$C_{n\beta} =$	-0.00161
$\Delta C_y (\delta_y = 90^\circ) =$	0.00786	$C_{y\delta_a} =$	0.00043
$C_{m\delta_e} =$	-0.0034	$C_{y\beta} =$	-0.0052
$C_{l\delta_a} =$	0.00143		

Vehicle Parameters

Wing Area	2690 sq ft
Wing Span	78.067 sq ft
Weight	195942.7 lb
Ixx	878620.8 slug -ft ²
Iyy	7160504.1 slug -ft ²
Body flap deflection	0.0°
Elevon deflection	0.0°

Trajectory Parameters

Altitude	209000 ft
Velocity	18477.2 ft/sec
Mach number	18.0
Dynamic pressure	70.266 lb/ft ²
Alpha	40°
Beta	0°

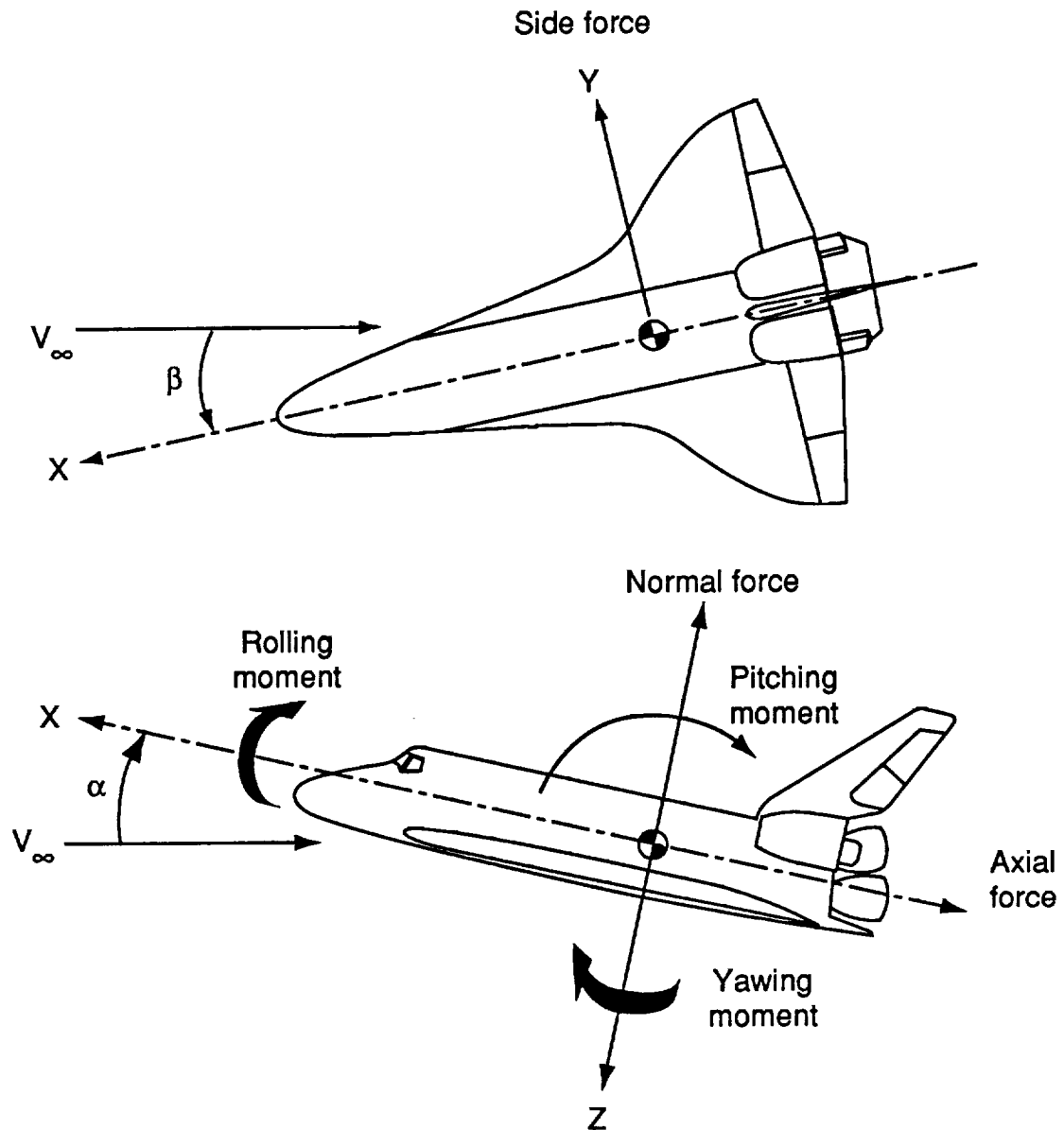


Figure 1. System of axes, showing positive direction of forces, moments, and angles.

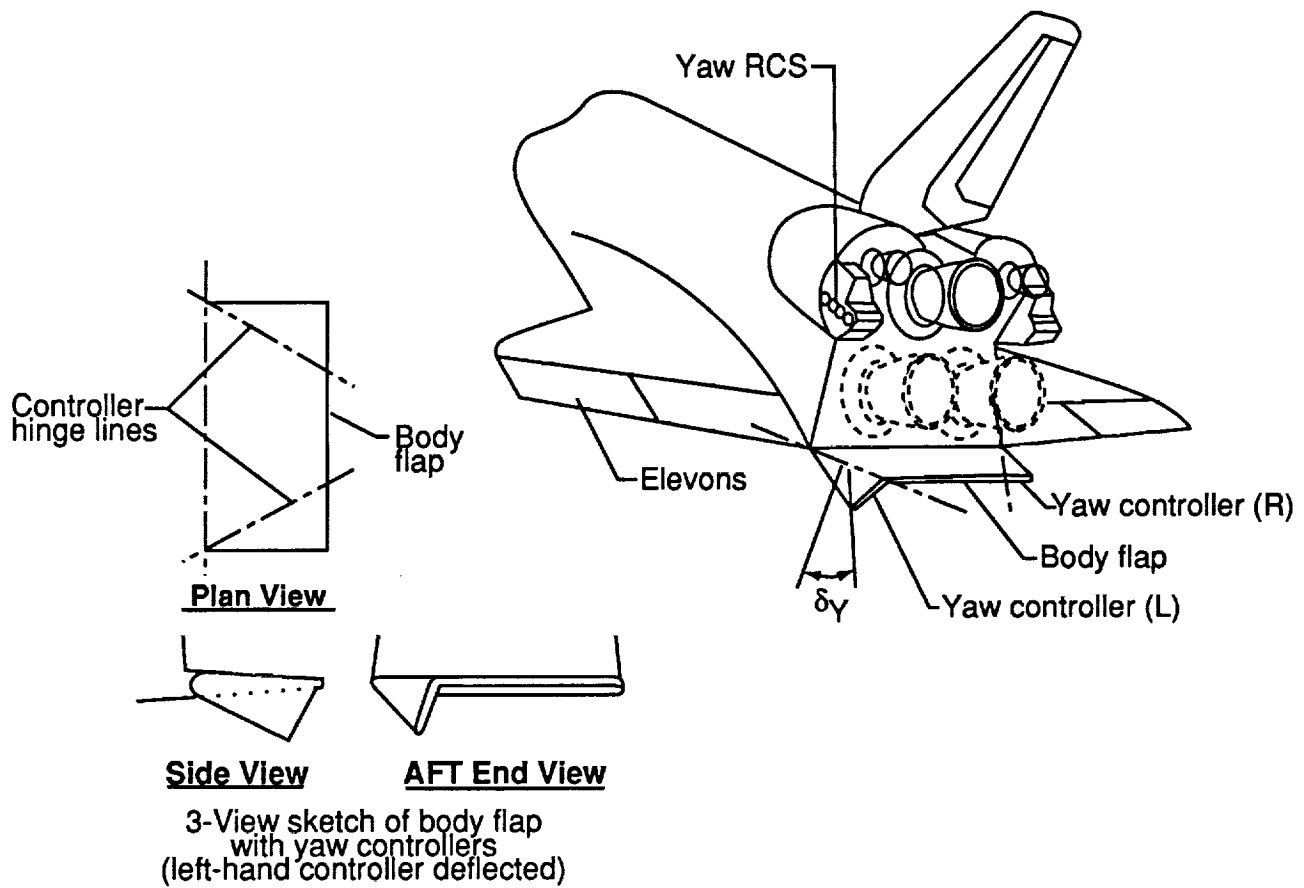


Figure 2. Sketch showing the yaw controller as applied to the Space Shuttle Orbiter.

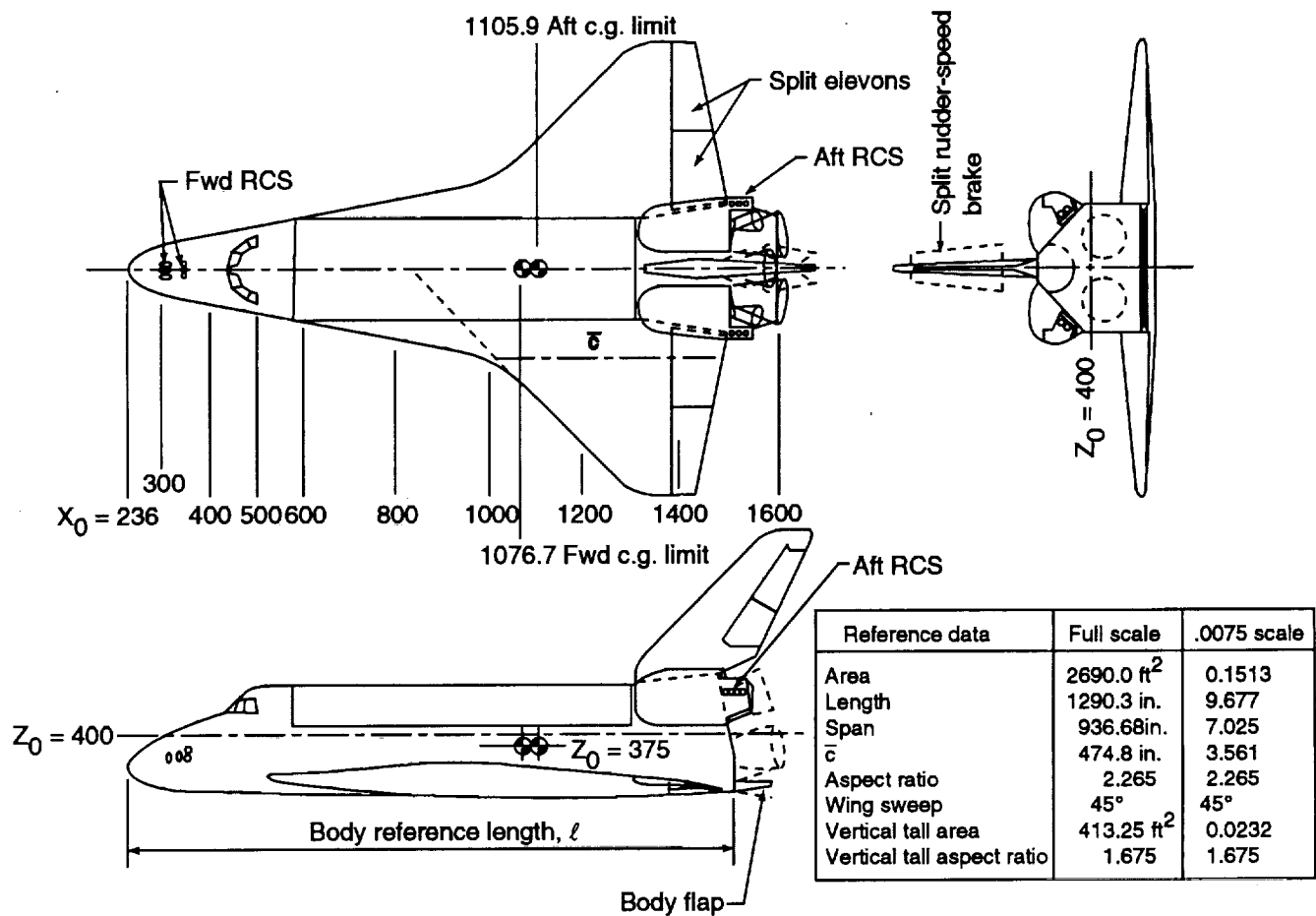


Figure 3. Three-view sketch of the orbiter configuration used in the investigation showing the full-scale and 0.0075 scale model dimensions. All dimensions are given in inches.

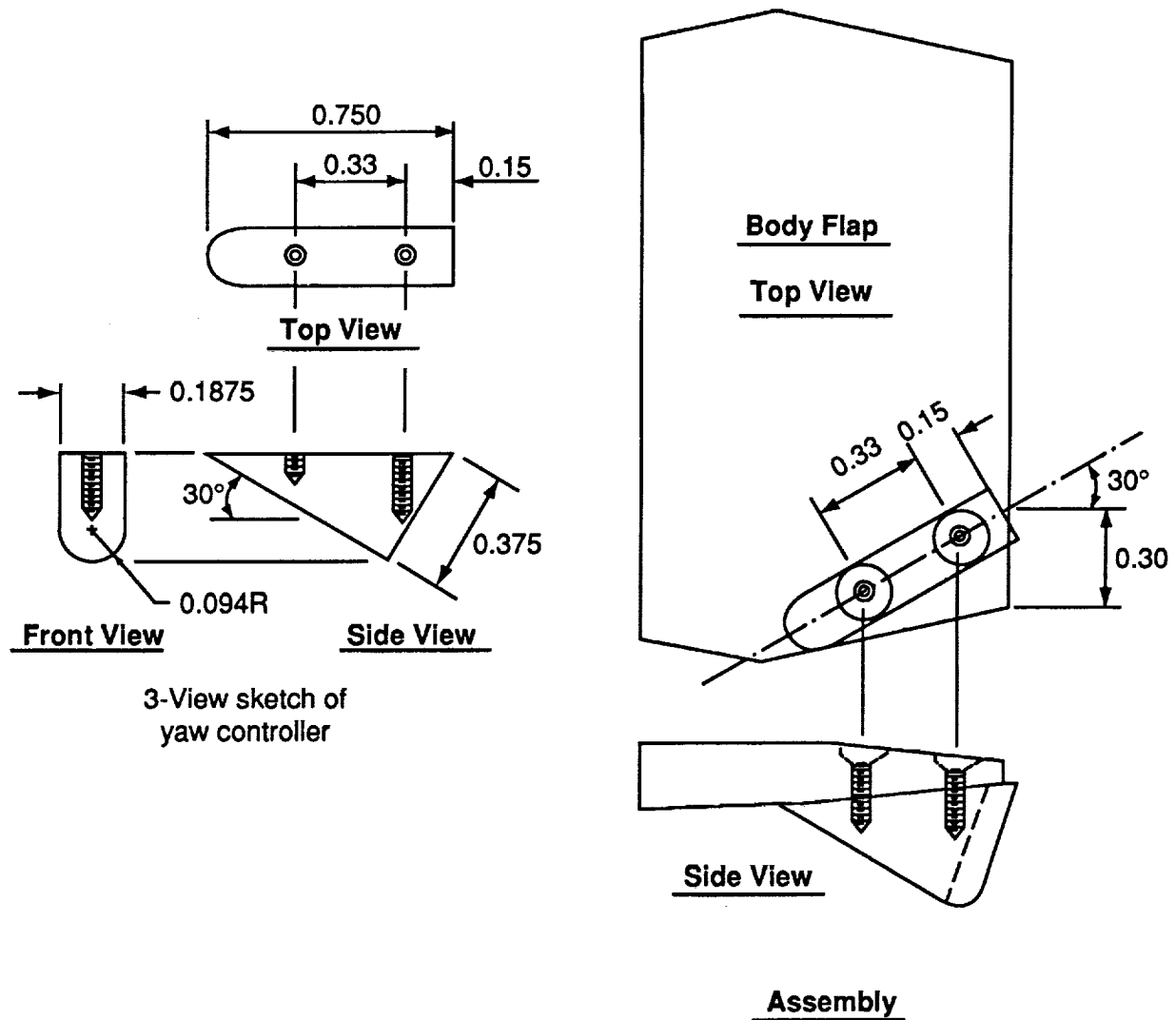


Figure 4. Sketch of yaw controller as built and tested, showing the pertinent dimensions and the arrangement when assembled. All dimensions are in inches.

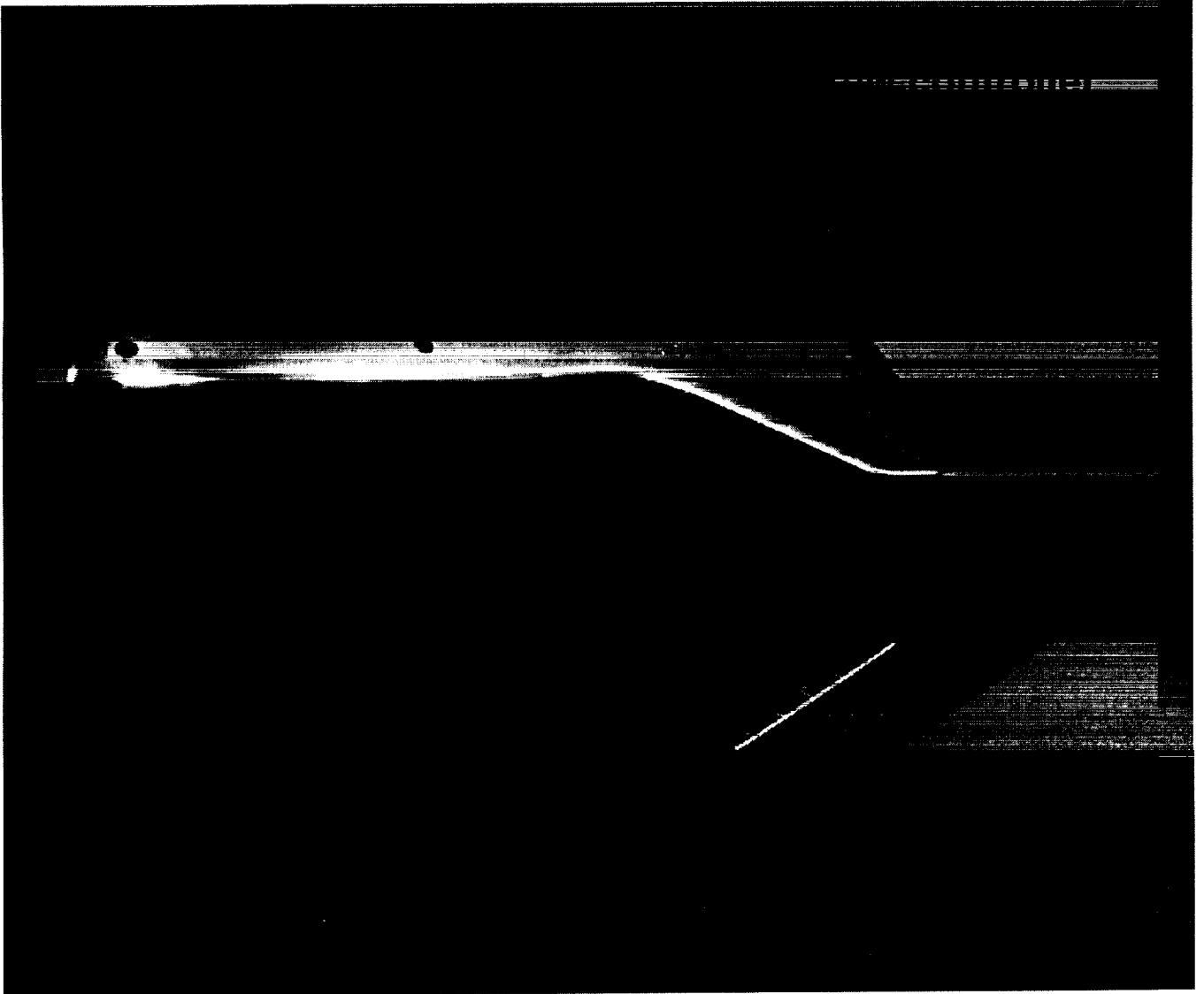
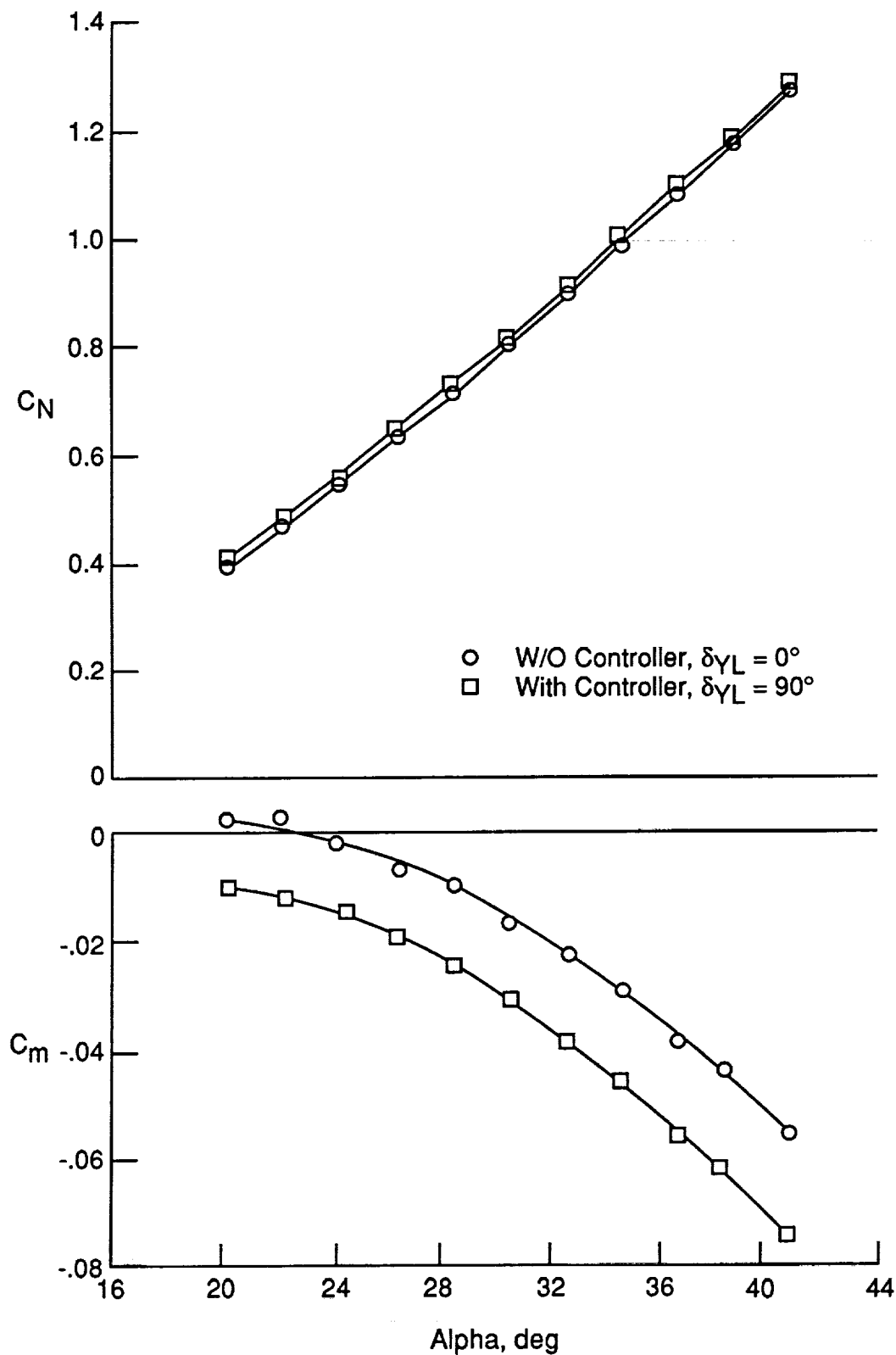
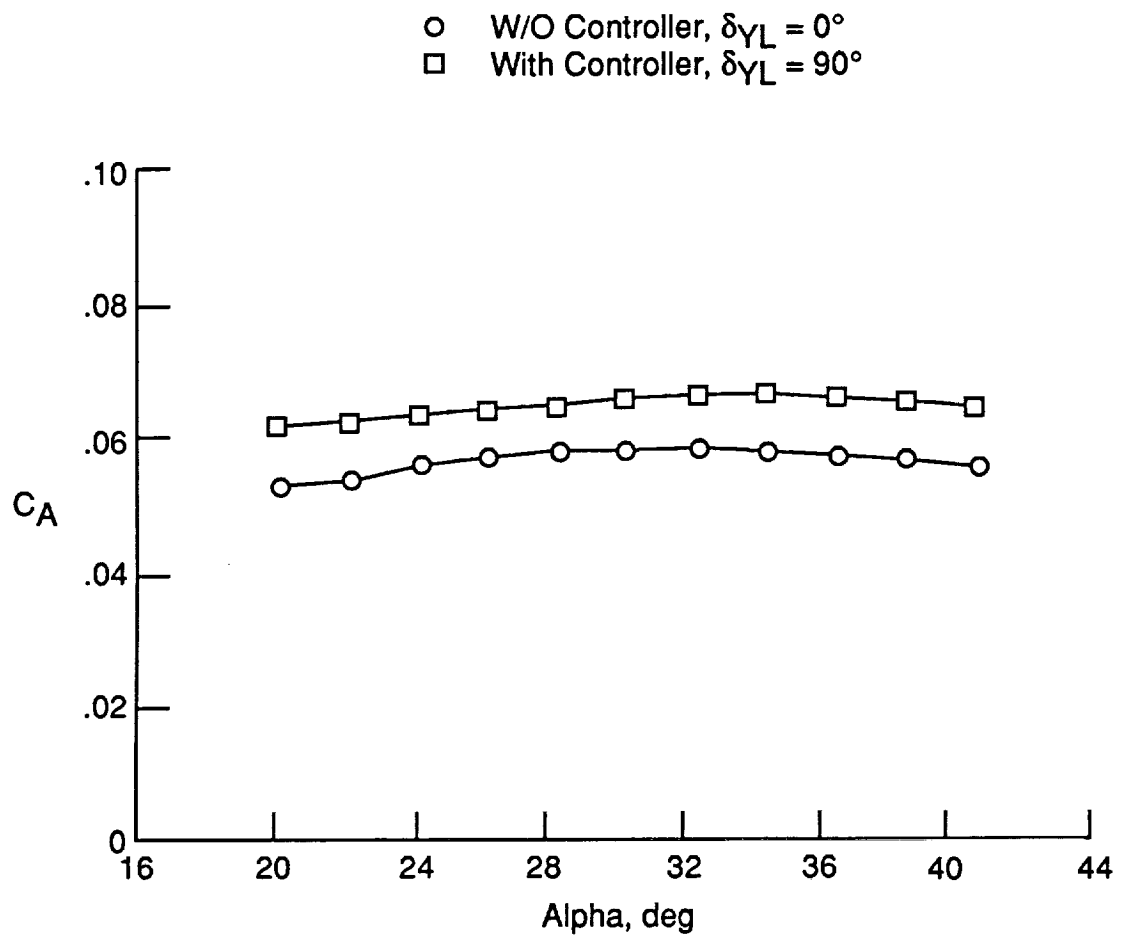


Figure 5. Photograph of the model with the yaw controller attached to the body flap.



(a) Normal force and pitching-moment coefficients.

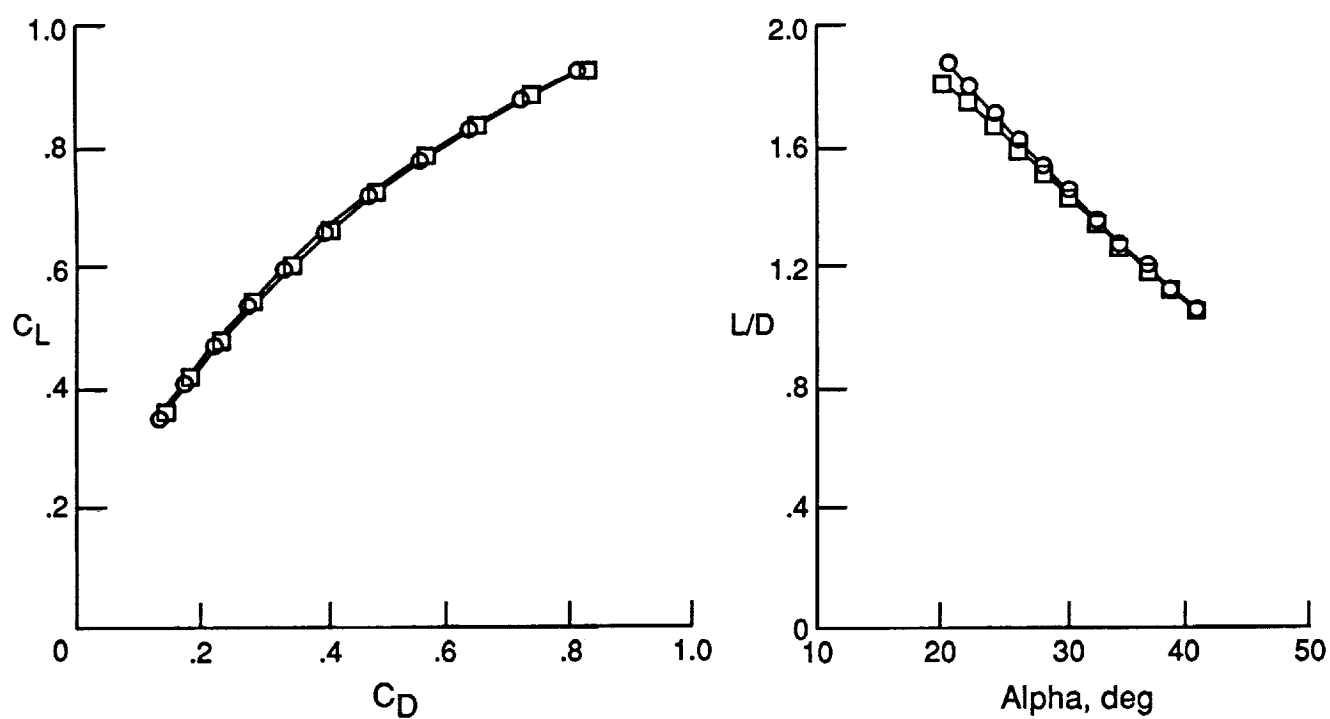
Figure 6. Effect of yaw controller on the static aerodynamic characteristics of the orbiter model. $R_\theta = 0.66 \times 10^6$.



(b) Axial force coefficient.

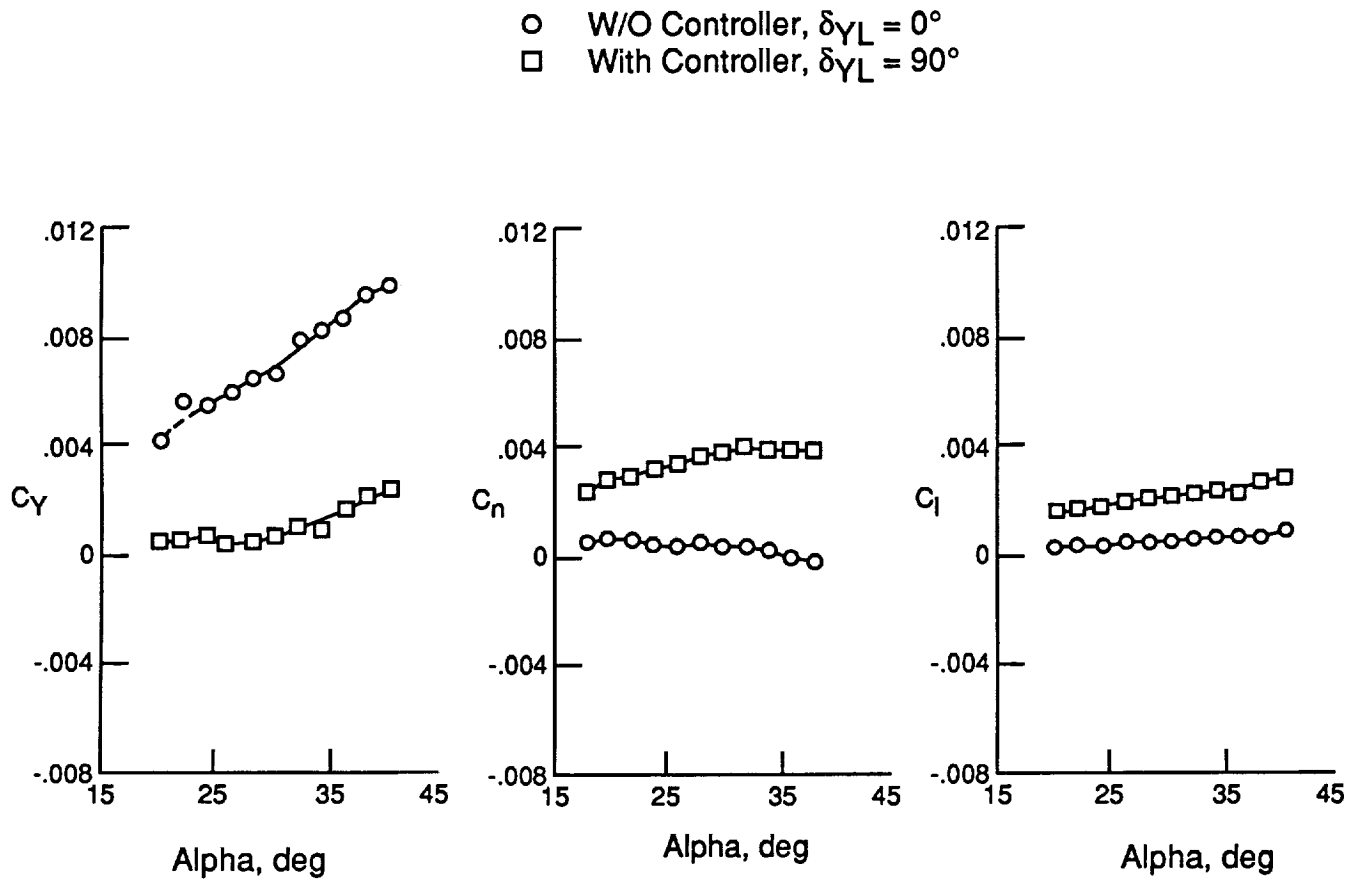
Figure 6. Continued.

- W/O Controller, $\delta\gamma_L = 0^\circ$
- With Controller, $\delta\gamma_L = 90^\circ$



(c) Lift, drag coefficients and L/D ratio.

Figure 6. Continued.



(d) Lateral aerodynamic characteristics.

Figure 6. Concluded.

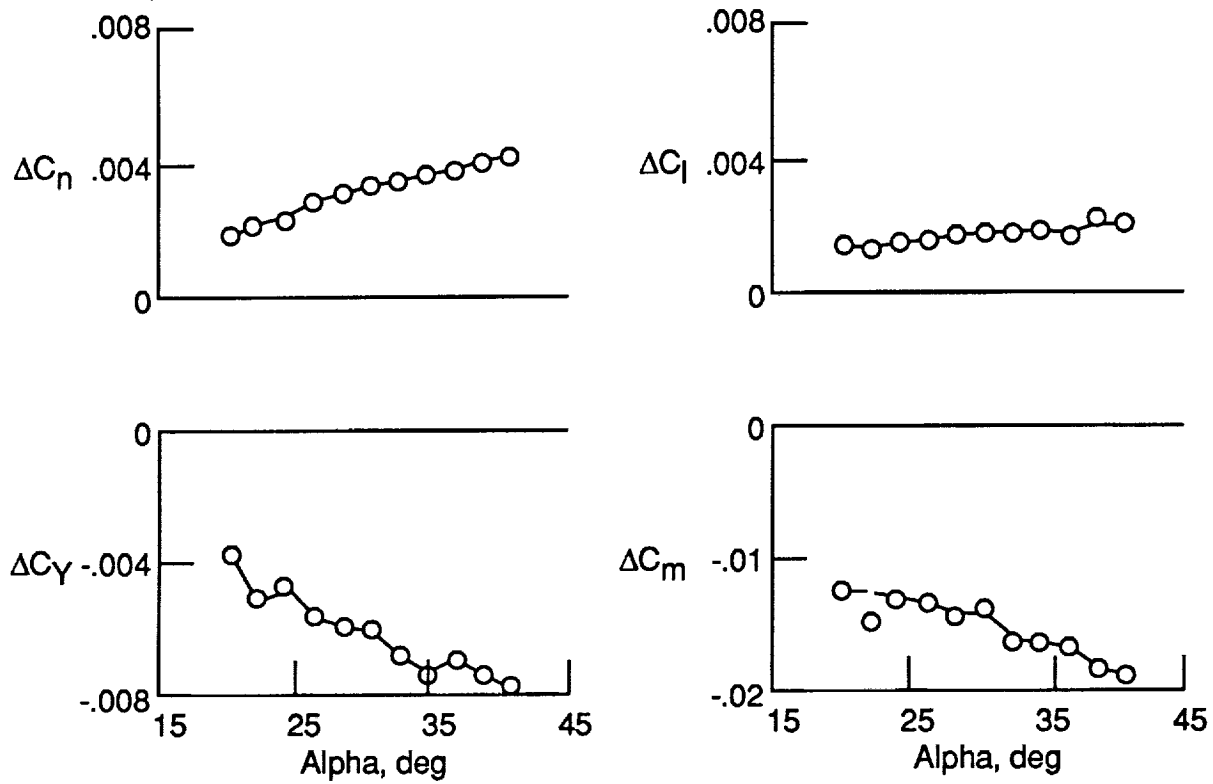


Figure 7. Variation of the incremental force and moment coefficients with angle of attack.

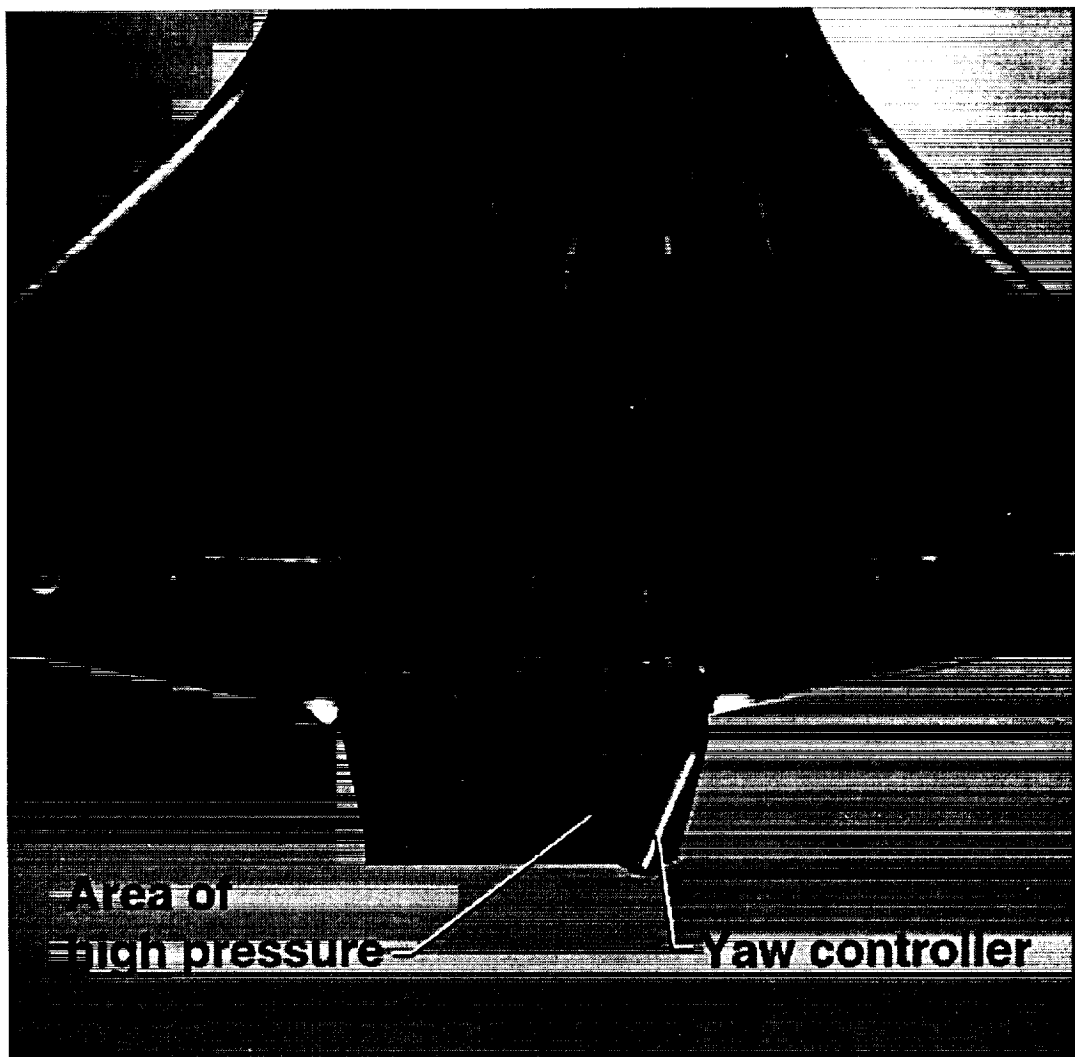


Figure 8. Surface oil-flow pattern on the bottom of the model with the controller installed, $\alpha = 40^\circ$.

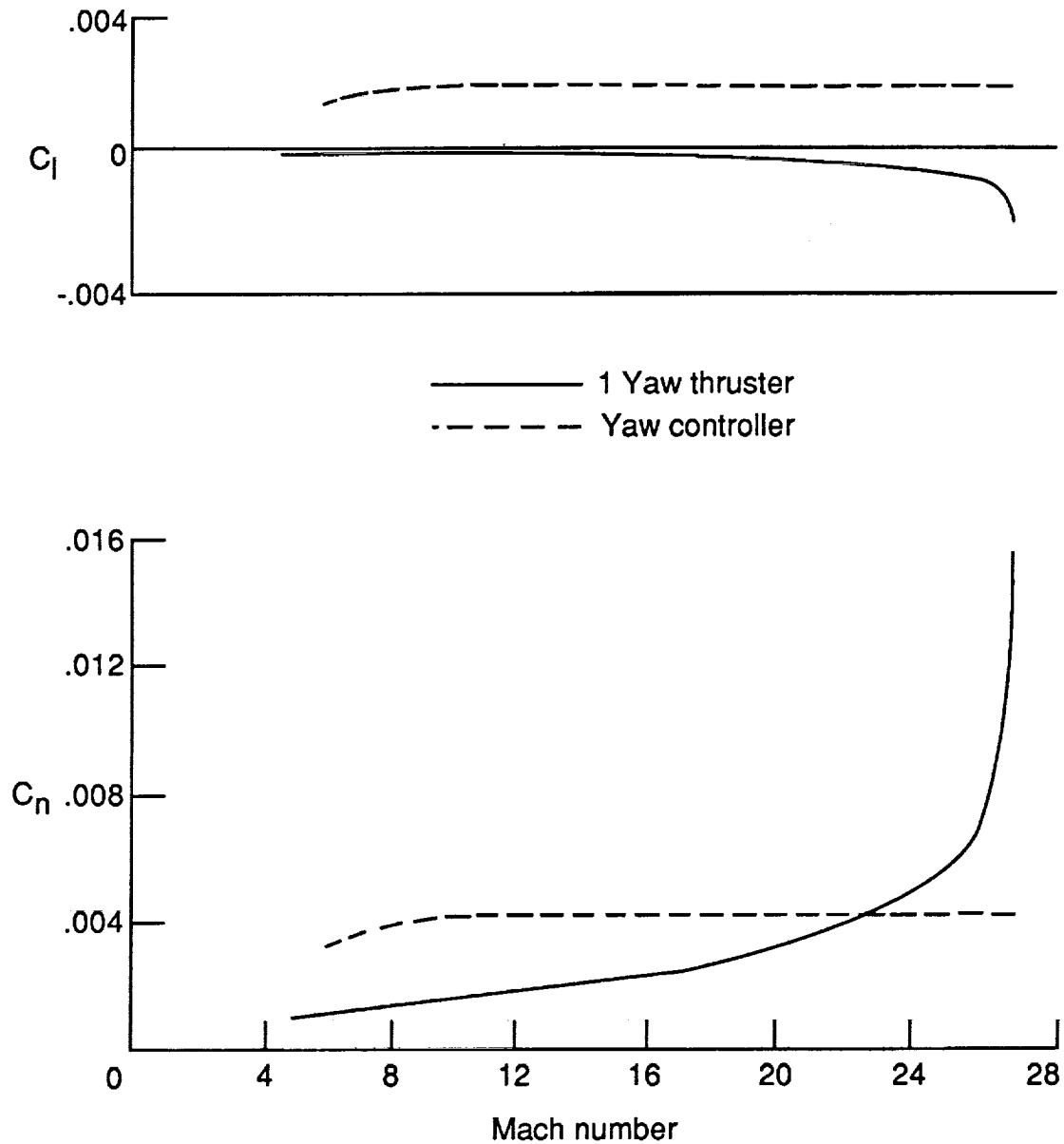


Figure 9. Comparison of the control effectiveness of the aerodynamic yaw controller with that of one RCS yaw thruster through a nominal entry trajectory from Mach 27 to Mach 4.

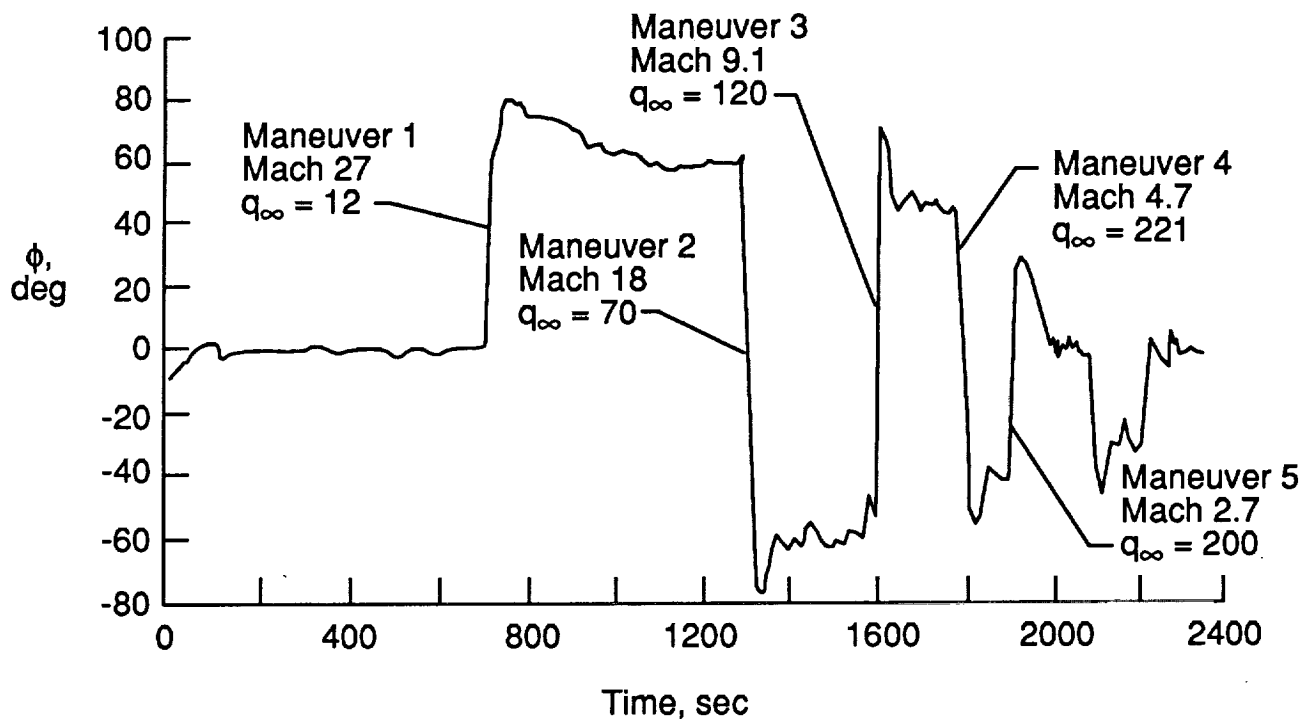
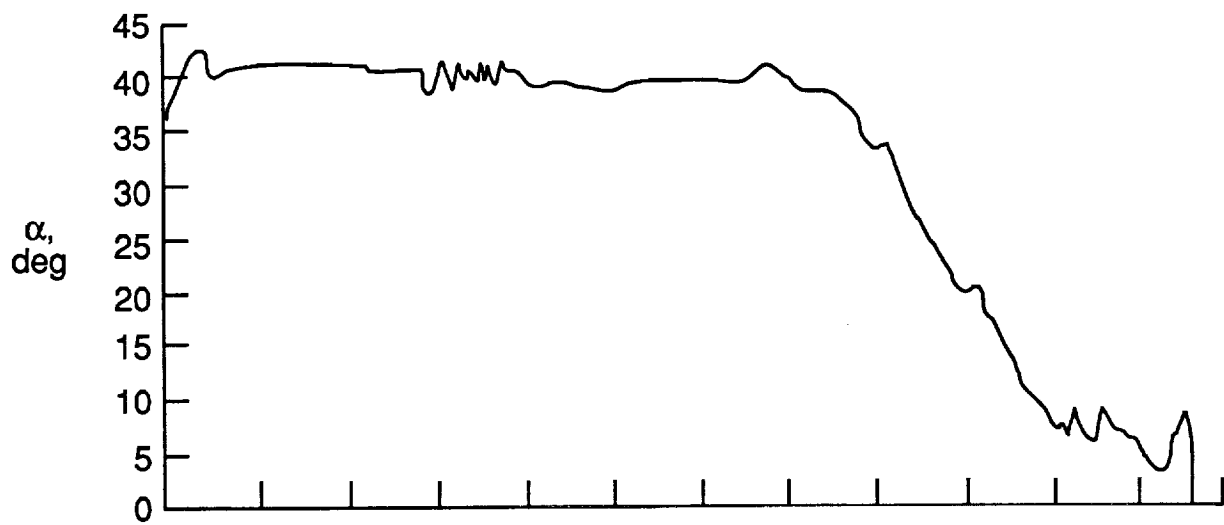


Figure 10. STS-1 entry showing bank maneuvers and angle of attack versus time.

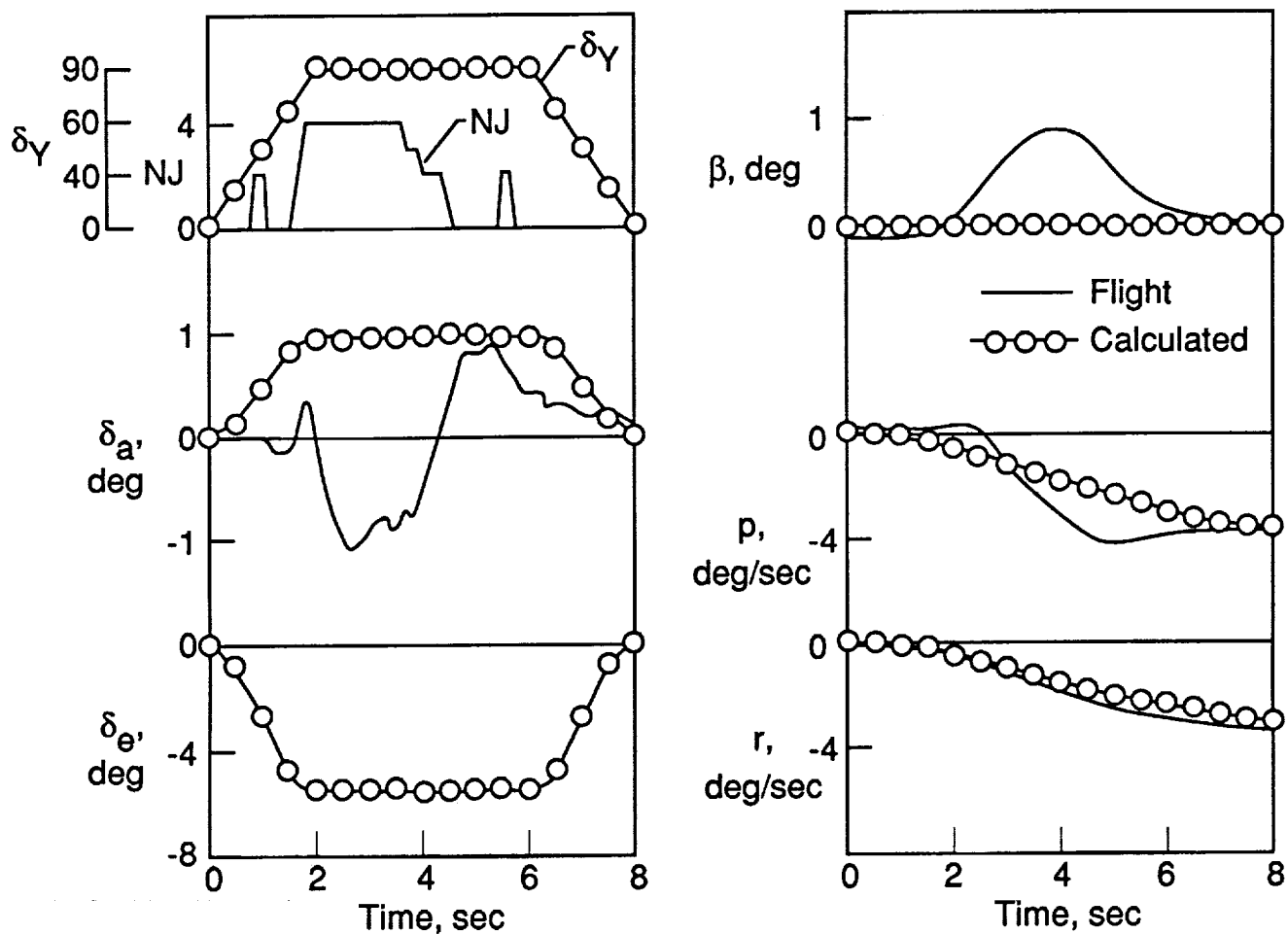


Figure 11. Comparison between calculations for the initiation of the STS-1 entry bank reversal at Mach 18 using the aerodynamic yaw controller with the actual flight maneuver. $H = 209,000$ ft., $V_\infty = 18,477$ ft./sec., $q_\infty = 70.26$ psf, $\alpha = 40^\circ$.

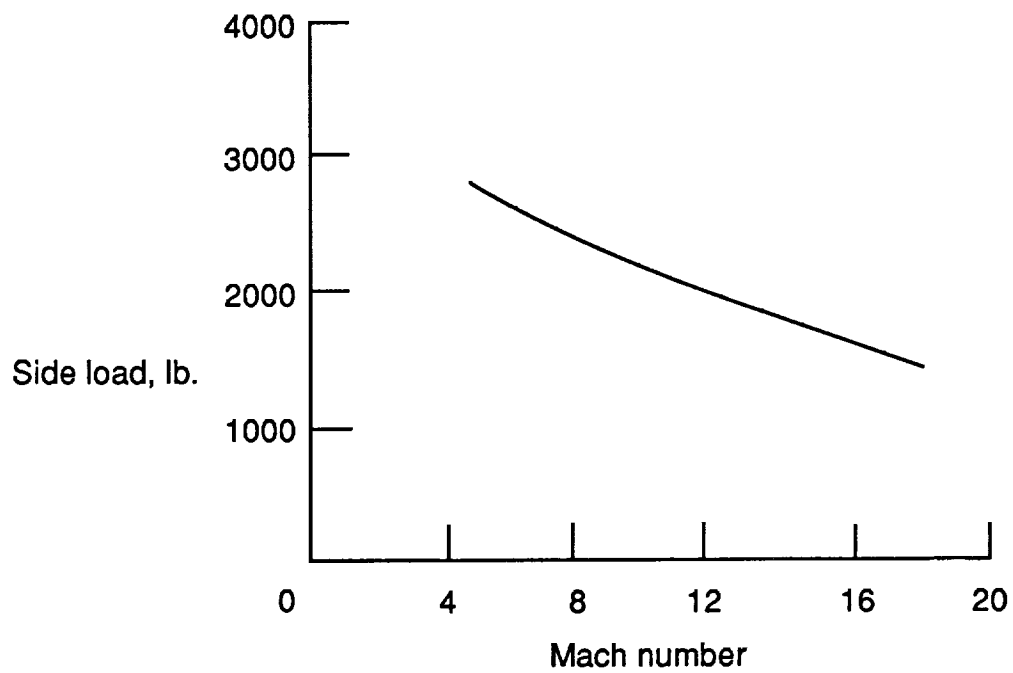


Figure 12. Variation of yaw controller/body flap side load with entry Mach number for the Orbiter STS-1 entry.

REPORT DOCUMENTATION PAGE

Form Approved
OMB No. 0704-0188

Public reporting burden for this collection of information is estimated to average 1 hour per response, including the time for reviewing instructions, searching existing data sources, gathering and maintaining the data needed, and completing and reviewing the collection of information. Send comments regarding this burden estimate or any other aspect of this collection of information, including suggestions for reducing this burden, to Washington Headquarters Services, Directorate for Information Operations and Reports, 1215 Jefferson Davis Highway, Suite 1204, Arlington, VA 22202-4302, and to the Office of Management and Budget, Paperwork Reduction Project (0704-0188), Washington, DC 20503.

1. AGENCY USE ONLY (Leave blank)		2. REPORT DATE February 1995	3. REPORT TYPE AND DATES COVERED Technical Memorandum
4. TITLE AND SUBTITLE Performance of an Aerodynamic Yaw Controller Mounted on the Space Shuttle Orbiter Body Flap at Mach 10			5. FUNDING NUMBERS 242-80-01-01
6. AUTHOR(S) W. I. Scallion			
7. PERFORMING ORGANIZATION NAME(S) AND ADDRESS(ES) NASA Langley Research Center Hampton, VA 23681-0001			8. PERFORMING ORGANIZATION REPORT NUMBER
9. SPONSORING / MONITORING AGENCY NAME(S) AND ADDRESS(ES) National Aeronautics and Space Administration Washington, DC 20546-0001			10. SPONSORING / MONITORING AGENCY REPORT NUMBER NASA TM-109179
11. SUPPLEMENTARY NOTES			
12a. DISTRIBUTION / AVAILABILITY STATEMENT Unclassified - Unlimited Subject Categories 02 and 15			12b. DISTRIBUTION CODE
13. ABSTRACT (Maximum 200 words) A wind-tunnel investigation of the effectiveness of an aerodynamic yaw controller mounted on the lower surface of a shuttle orbiter model body flap was conducted in the Langley 31-Inch Mach 10 Tunnel. The controller consisted of a 60° delta fin mounted perpendicular to the body flap lower surface and yawed 30° to the free stream direction. The control was tested at angles of attack from 20° to 40° at zero sideslip for a Reynolds number based on wing mean aerodynamic chord of 0.66 x 10/6. The aerodynamic and control effectiveness characteristics are presented along with an analysis of the effectiveness of the controller in making a bank maneuver for Mach 18 flight conditions. The controller was effective in yaw and produced a favorable rolling moment. The analysis showed that the controller was as effective as the reaction control system in making the bank maneuver. These results warrant further studies of the aerodynamic/aerothermodynamic characteristics of the control concept for application to future transportation vehicles.			
14. SUBJECT TERMS orbiter, aerodynamics, control			15. NUMBER OF PAGES 28
			16. PRICE CODE A03
17. SECURITY CLASSIFICATION OF REPORT Unclassified	18. SECURITY CLASSIFICATION OF THIS PAGE Unclassified	19. SECURITY CLASSIFICATION OF ABSTRACT	20. LIMITATION OF ABSTRACT